LUND UNIVERSITY
Faculty of Science

Evaluation of light scattering and absorption in aerosol nanowires

Yoana Ilarionova

Thesis submitted for the degree of Bachelor of Science
Project duration: 2 months

Supervised by Martin Magnusson and Yang Chen

Department of Physics
Division of Solid State Physics
January 2019

Contents

Abstract

Numerical models of the optical properties of a single nanowire are essential for reproducing the results of the measurements and understanding the optical processes. Intuitively, the properties of a single finitely long nanowire would converge to the ones for an infinitely long nanowire if it is long enough. However, the simulations show that the scattering cross section per unit length of a finitely long nanowire is better approximated by the cross section per unit length of another finitely long wire with a different length than by an infinitely long nanowire, which reduces the degrees of freedom by one. The results regarding the infinitely long nanowires were based on Mie scattering, while the ones concerning the finitely long nanowires were based on the discrete dipole approximation.

Chapter 1

Introduction

In the recent years nanoscience has been a rapidly developing field of natural science and one of its most promising achievements is the design and production of semiconductor nanowires(see fig. 1.1). These are structures with diameters in the order of tens of nanometers and a typical length of a few micrometers. They can be grown from a seed particle (usually gold) in a gas chamber where the materials are introduced in the form of gas.

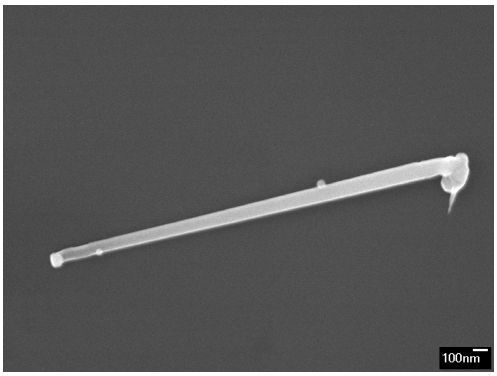

(a) Image of a GaAs nanowire taken with scanning electron microscope (SEM). Nanowires grown by Sudhakar Sivakumar; the image was taken by Marcus Tornberg.

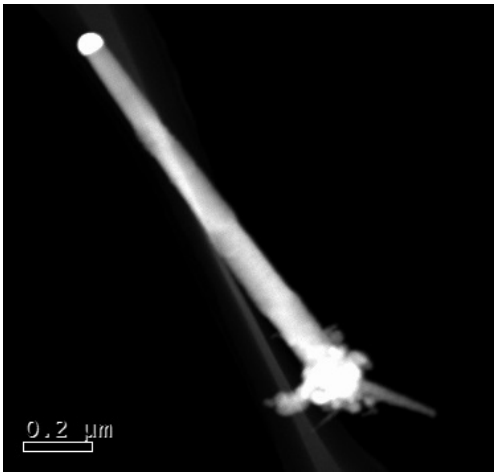

(b) Dark field image of a GaAs nanowire doped with Sn taken with transmission electron microscope (TEM). Nanowires were grown by Sudhakar Sivakumar and prepared for TEM by Axel Persson; the image was taken by Calle Preger.

Figure 1.1: Images of GaAs nanowires taken with a)SEM and b)TEM. Both are unpublished. The people involved are part of the division of solid state physics, department of physics, Lund university, except Axel Persson who is a part of the centre for analysis and synthesis, department of chemistry, Lund university.

There are two methods to grow nanowires depending on whether using a substrate or not. In the first one, seed particles are placed on a wafer and the wafer is placed in a growth chamber with metalorganic gas flows. These gases dissolve in the gold particle and finally crystallize on the substrate. That method is called the vapor-liquid-solid method or metalorganic vapor-phase epitaxy [1]. The other method requires sending the seed particles through the reaction chambers as an aerosol without a substrate and the growth rate is much higher. This method is known as aerotaxy [2]. Semiconductor devices such as nanowire array solar cells [3, 4, 5, 6], photodetectors [7, 8] and LEDs [6] can be fabricated based with these growth

methods.

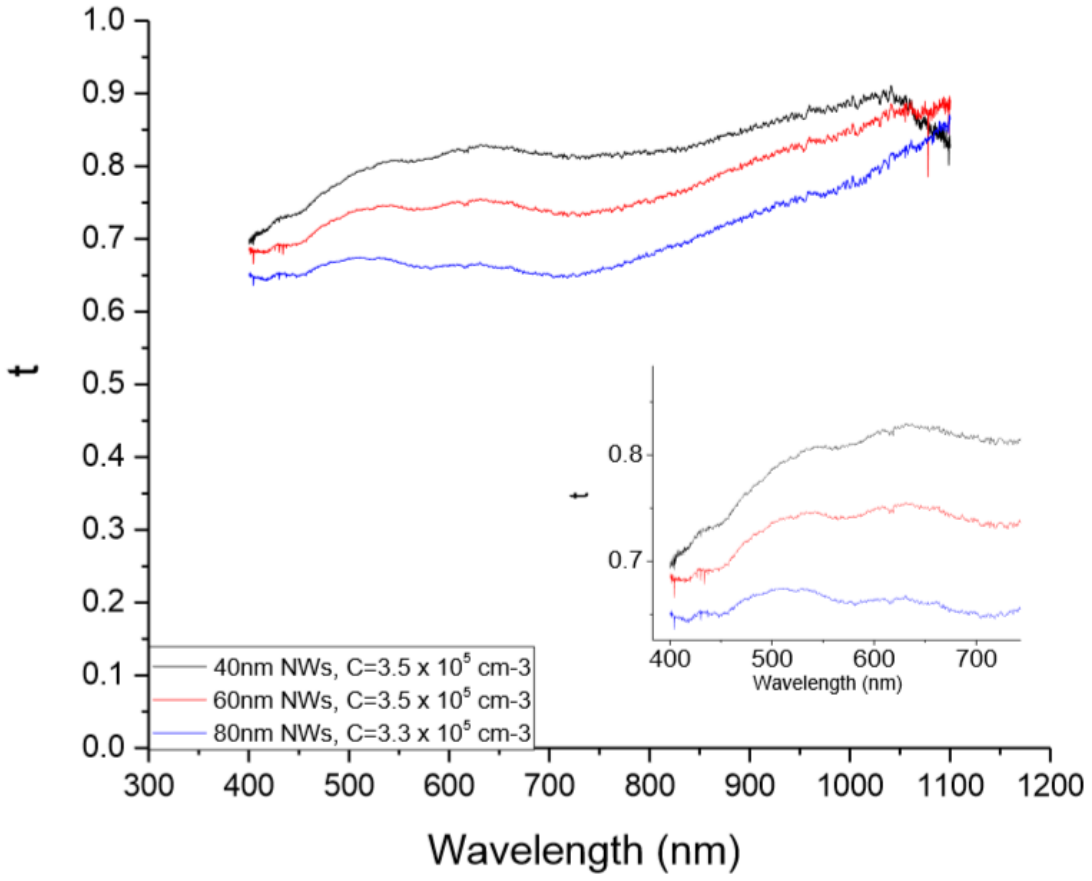

Figure 1.2: The transmission spectra of low-concentration GaAs nanowires. t is the live transmission normalized to the blank reference spectrum. The figure was taken from Eleni Gompou's master thesis [9].

To study the optical response of aerotaxy nanowires, a setup1.3 has been built to obtain the transmission spectrum of GaAs nanowires with gold seed particle in the air. An example is shown in fig. 1.2 [9] but the physical property of transmission is still unclear. There is also an attempt to simulate such spectra in order to improve the understanding. One simulation of the scattering by a single nanowire takes about 18 minutes but it has to be repeated for nanowires with different lengths, diameters and orientations. For aerotaxy nanowires, diameters typically range from 20 to 120 nm, so if the diameter is varied in steps of 5 nm, that gives 21 diameters considered. Moreover, the length is varied from 100 to 3000 nm in steps of 100 nm, so 30 options in total. Furthermore, the orientations are given by the polar angle and the azimuth. The polar angle has a range from 0 to 360 degrees, while the azimuth has a range of 0 to 180 degrees. If both are varied in steps of 5 degrees, the resulting options would be 72 and 36 respectively. The total number of simulations is $21 \cdot 30 \cdot 72 \cdot 36 = 1632960$ simulations, which would require $18 \cdot 1632960 = 293932800$ minutes or 489888 hours or 20412 days, that is approximately 56 years.

It is possible to decrease the computation time to a few months by numerical alternatives and symmetries but this is still an unacceptably long time. However, there is a possibility that an analytic approximation can speed up the calculation.

In Physics, approximating a parameter to infinity simplifies the problem, e. g. a crystal band diagram is usually considered based on an infinite crystal even if it has dimensions of a few micrometers. Similarly, if the length of a nanowire can be approximated as an infinitely long cylinder, the computation time is

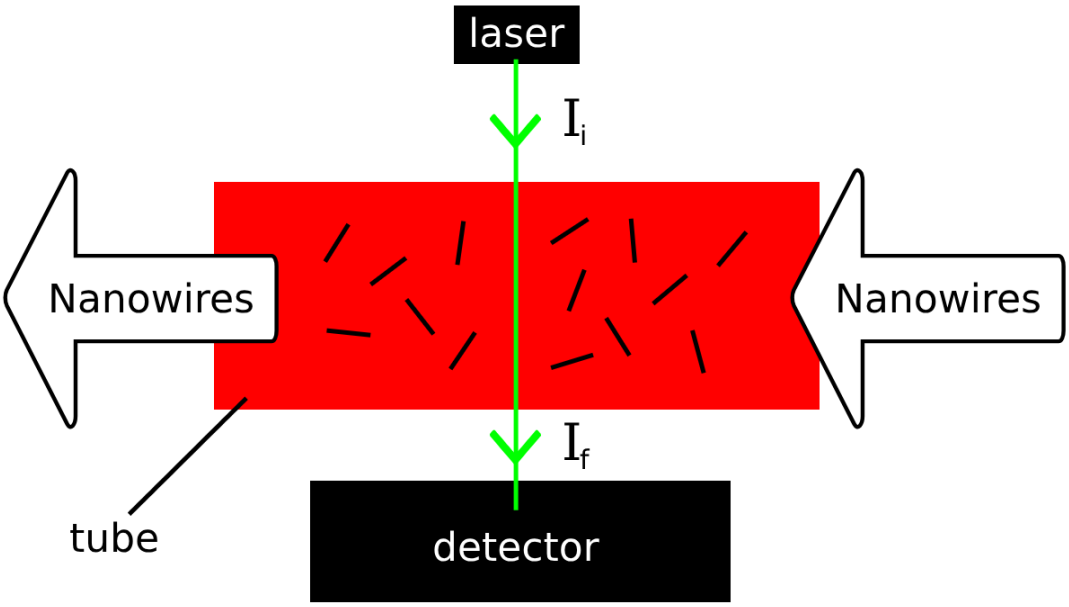

Figure 1.3: A simplified version of the set up used by Eleni Gompou for obtaining the spectra on fig.1.2. I_i is the intensity of the incoming laser light and I_f is the intensity of the light coming out of the tube, having traveled distance l. According to Beer-Lambert law, $I_f = I_i e^{-\sigma_e N l}$ where σ_e is the extinction cross section and $\sigma_e = \sigma_s + \sigma_a$ where σ_s is the scattering cross section and σ_a is the absorption cross section.

going to decrease enormously because an infinite cylinder interacting with light has an analytic solution which is known as Mie scattering [10].

In this thesis, the main focus is the validity of using Mie theory to simulate finitely long nanowires. The assessment is done by varying the length and the diameter of the nanowires and comparing the far-field plot and the scattering cross section per unit length.

Chapter 2

Theory and Method

In optics, light can be treated either as a ray or as an electromagnetic wave. However, when the size of the structure is comparable to the wavelength of light, the wave behavior dominates.

The likelihood of light interacting an object is represented by its extinction cross section σ_e, which the sum of the scattering σ_s and the absorption cross section σ_a.

The optical response of a system can be described by the solutions of Maxwell's equations:

$$\nabla \cdot \vec{E} = \frac{\rho}{\varepsilon_0} \tag{2.1}$$

$$\nabla \cdot \vec{B} = 0 \tag{2.2}$$

$$\nabla \times \vec{E} = -\frac{\partial \vec{B}}{\partial t} \tag{2.3}$$

$$\nabla \times \vec{B} = \mu_0 \left(\vec{J} + \varepsilon_0 \frac{\partial \vec{E}}{\partial t} \right) \tag{2.4}$$

Here $\vec{E}$ is the electric field, $\vec{J}$ is the current density and $\vec{B}$ is the magnetic field.

These equations can be solved for a small spherical particle or for an infinitely long nanowire. These solutions are also known as the Mie scattering [10]. For a particle, the scattering cross section is normalized by the geometric cross section to form the scattering cross efficiency, which can be interpreted as scattering cross section per unit area and is unitless. However, for infinitely long cylinder, the scattering cross section efficiency is the scattering cross section per unit length normalized by the geometric cross section per unit length.

2.1 Mie Scattering

In Mie scattering, the size of the particles or the diameter of the nanowire should be comparable to the light wavelength, or at the nanoscale. However, a big object can be represented by a collection of small particles. The amplitude of the scattered electric field can be directly derived from the intensity of the incident field [11]:

$$\begin{bmatrix} E_{\parallel s} \\ E_{\perp s} \end{bmatrix} = \frac{e^{ik(r-z)}}{-ikr} \begin{bmatrix} S_2 & S_3 \\ S_4 & S_1 \end{bmatrix} \begin{bmatrix} E_{\parallel i} \\ E_{\perp i} \end{bmatrix} \tag{2.5}$$

Here $E_{\parallel s}$ and $E_{\perp s}$ are the parallel and the perpendicular component of the scattered electric field with respect to the scattering plane and $E_{\parallel i}$ and $E_{\perp i}$ are the parallel and the perpendicular component

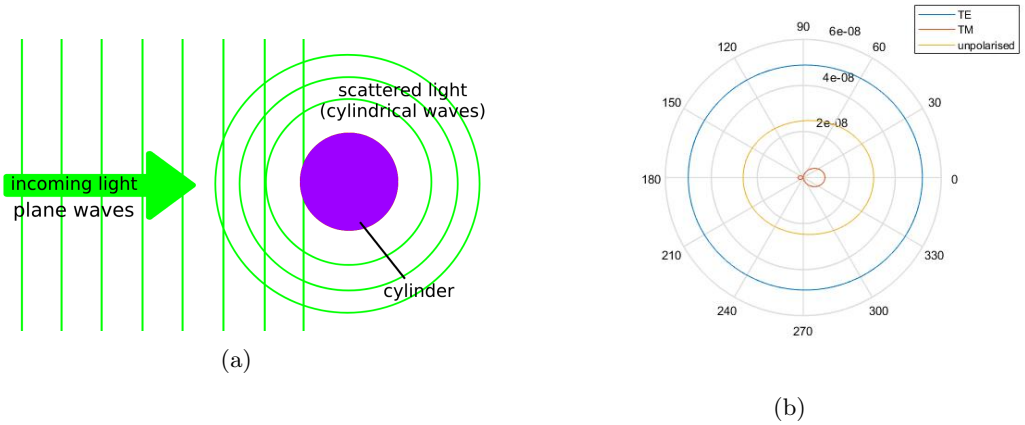

(a) (b)

Figure 2.1: (a) A schematic depiction of a scattering from a cylinder, seen from the positive z-direction. The lines represent the wave fronts - planes for the incoming wave and cylindrical for the scattered wave. (b) The differential scattering scattering cross section in arbitrary units vs. angle for an infinitely long nanowire with a diameter of 80 nm; viewed from the axis of the nanowire, done with Matscat.

of the incident electric field. The $S_j(j = 1, 2, 3, 4)$ are the elements of the amplitude scattering matrix and they depend on the scattering angle θ and the azimuthal angle ϕ [11].

The Stokes parameters of the scattered light can be calculated as [11]:

$$I_s = \langle E_{\parallel s} E^*_{\parallel s} + E_{\perp s} E^*_{\perp s} \rangle \tag{2.6}$$

$$Q_s = \langle E_{\parallel s} E^*_{\parallel s} - E_{\perp s} E^*_{\perp s} \rangle \tag{2.7}$$

$$U_s = \langle E_{\parallel s} E^*_{\perp s} + E_{\perp s} E^*_{\parallel s} \rangle \tag{2.8}$$

$$V_s = i\langle E_{\parallel s} E^*_{\perp s} - E_{\perp s} E^*_{\parallel s} \rangle \tag{2.9}$$

The relationship between the Stokes parameters of the incident and the scattered light is given by the following equation [11]:

$$\begin{bmatrix} I_s \\ Q_s \\ U_s \\ V_s \end{bmatrix} = \frac{1}{k^2 r^2} \begin{bmatrix} S_{11} & S_{12} & S_{13} & S_{14} \\ S_{21} & S_{22} & S_{23} & S_{24} \\ S_{31} & S_{32} & S_{33} & S_{34} \\ S_{41} & S_{42} & S_{43} & S_{44} \end{bmatrix} \begin{bmatrix} I_i \\ Q_i \\ U_i \\ V_i \end{bmatrix} \tag{2.10}$$

Here each $S_{i,j}$ is directly derived from the elements of the amplitude scattering matrix.

The scattering cross section efficiency Q_{scat} is given as [11]:

$$Q_{scat} = \frac{1}{x} \left[|b_{0\mathrm{I}}|^2 + 2 \sum_{n=1}^{\infty} (|b_{n\mathrm{I}}|^2 + |a_{n\mathrm{I}}|^2) + |a_{0\mathrm{II}}|^2 + 2 \sum_{n=1}^{\infty} (|a_{n\mathrm{II}}|^2 + |b_{n\mathrm{II}}|^2) \right] \tag{2.11}$$

where a_i and b_i the scattering coefficients and as:

$$Q_{scat} = \frac{C_{scat}}{G} \tag{2.12}$$

where C_{scat} is the scattering cross section of the nanowire per unit length and G is the geometric cross section of the nanowire per unit length.

2.2 Discrete Dipole Approximation

The discrete dipole approximation is used to solve the interaction between a finitely long nanowire and light. The nanowire is divided into cubes with sides of 5 nm. The dipole moments of the cubes are calculated according to the material parameter. The superposition of all those interacting with the light represents the interaction of the nanowire with the light which makes it possible to calculate the total scattering cross section C_s, since the wire is not infinitely long. The scattering cross section per unit length C_{scat} for a nanowire with length L is then equal to:

$$C_{scat} = \frac{C_s}{L} \tag{2.13}$$

2.3 Method

The comparison between the infinitely long nanowire approximation and the realistic finitely long nanowires is done by simulating the near-field pattern, the scattering cross section per unit length and estimating the differences. The characteristics of the infinitely long nanowire were calculated for diameters between 20 and 120 nm in steps of 5 nm. The behaviour of the finitely long nanowires was calculated for wires with the same diameter sweep and length from 100 to 3000 nm in steps of 100 nm.

The simulations for the infinitely long nanowires were done with the MatScat package based on the Huffman's [11] and Kerker's [12] books. The near-field pattern was obtained using the formulas in Huffman's book, while the scattering cross section per unit length was based on Kerker's. The calculations were then confirmed with the finite element method [13] by COMSOL Multiphysics.

The simulations of the scattering cross section per unit length for the finitely long nanowire were done with DDScat using the discrete dipole approximation. The simulations of the near-field pattern shown in section 3.1 were done with COMSOL Multiphysics.

Chapter 3

Results

Near-field pattern and scattering cross section per unit length of the infinitely and finitely long wires were compared. The simulations concerning infinitely long nanowires were done for GaAs nanowires with refractive index n given in table 3.1, the rest of the simulations were done for GaAs nanowires with complex refractive index, found with interpolation. However, the imaginary part of the refractive index is significantly smaller than the real part, so the absorption cross section is sufficiently smaller then the scattering cross section.

Table 3.1: Table of the used refractive indices

Software	Refractive index n	Simulations done with the software
COMSOL (Mie scattering model)	3.5	near-field simulations
Matscat (Mie scattering model)	3.5	cross section calculation
COMSOL (Finitely long nanowire model)	$4.1 + 0.32i$	near-field simulations
DDScat (DDS)	$4.1 + 0.32i$	cross section calculation

3.1 Near-field pattern

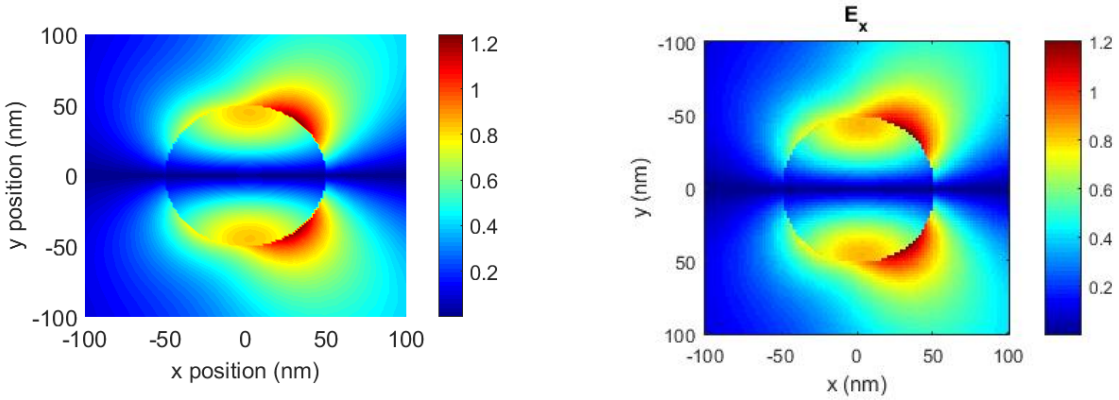

(a) (b)

Figure 3.1: The x-component E_x of the electric field (a) (incoming plus scattered) according to the COMSOL simulation (plotted with Matlab) and (b) (scattered only) according to the Matscat simulation, calculated for an infinitely long nanowire with a diameter of 100 nm.

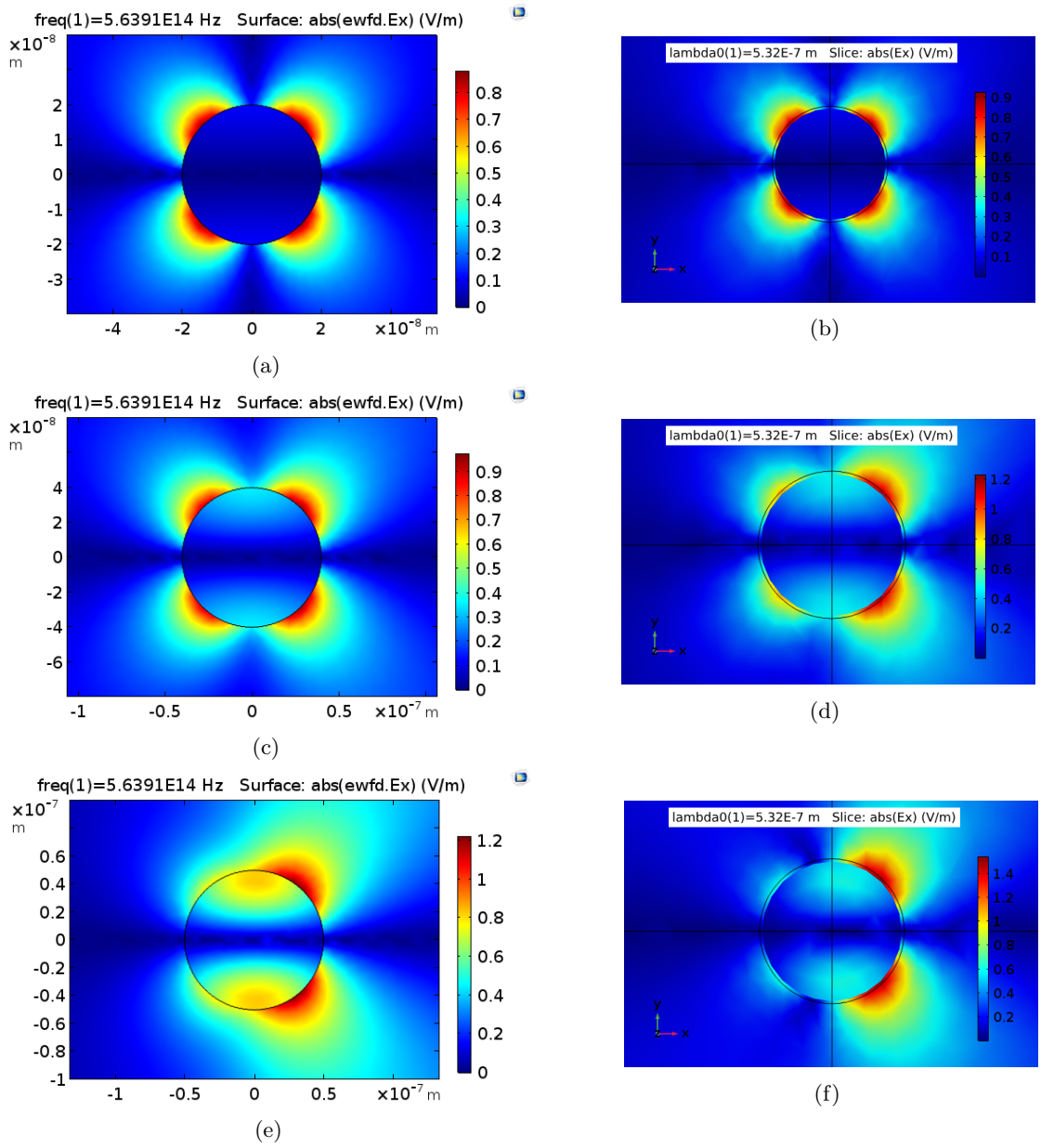

Figure 3.2: Color plot of the E_x field of (a, c, e) an infinitely long nanowire and (b, d, f) a 2 µm long nanowire with a diameter of (a, b) 40, (b, c) 80 and (e, f) 100 nm. The values of E_x are represented by the color in all figures.

The near-field patterns of the infinite nanowires for perpendicular incidence were calculated by both COMSOL and Matscat, both using Mie scattering (ch.2), for wires with diameter of 40, 80 and 100 (fig.3.1). The results confirmed that the numerical approximations are good. Therefore, it is sufficient to use only one of them.

The near-field pattern is represented by the x-component of the electric field since the incoming light was linearly polarized in the y-direction propagating in the x-direction. Therefore, the x-component of the electric field of the incoming wave is zero.

The near-field pattern was obtained for 2 µm long nanowires with diameters of 40, 80 and 100 nm with COMSOL (fig.3.2). The displayed values concern E_x in the xy plane through the origin, perpendicular to the symmetry axis of the nanowire. The near-field pattern seems to match for the nanowires with 40 nm

diameter but for the ones with 80 and 100 nm, there are some differences. In order to investigate whether the match would improve with length, since the longer the wire is the closer it is to infinitely long, the near-field pattern was obtained for nanowires with the same diameters and length of 1 and 3 µm (fig.3.3). All of the obtained patterns are symmetric with respect to the xz-plane but the ones corresponding to nanowires with diameter of 40 nm are also symmetric with respect to the yz-plane. However, there was no significant in the near-field patterns and therefore, they did not match better than the ones for the 2 µm long nanowires.

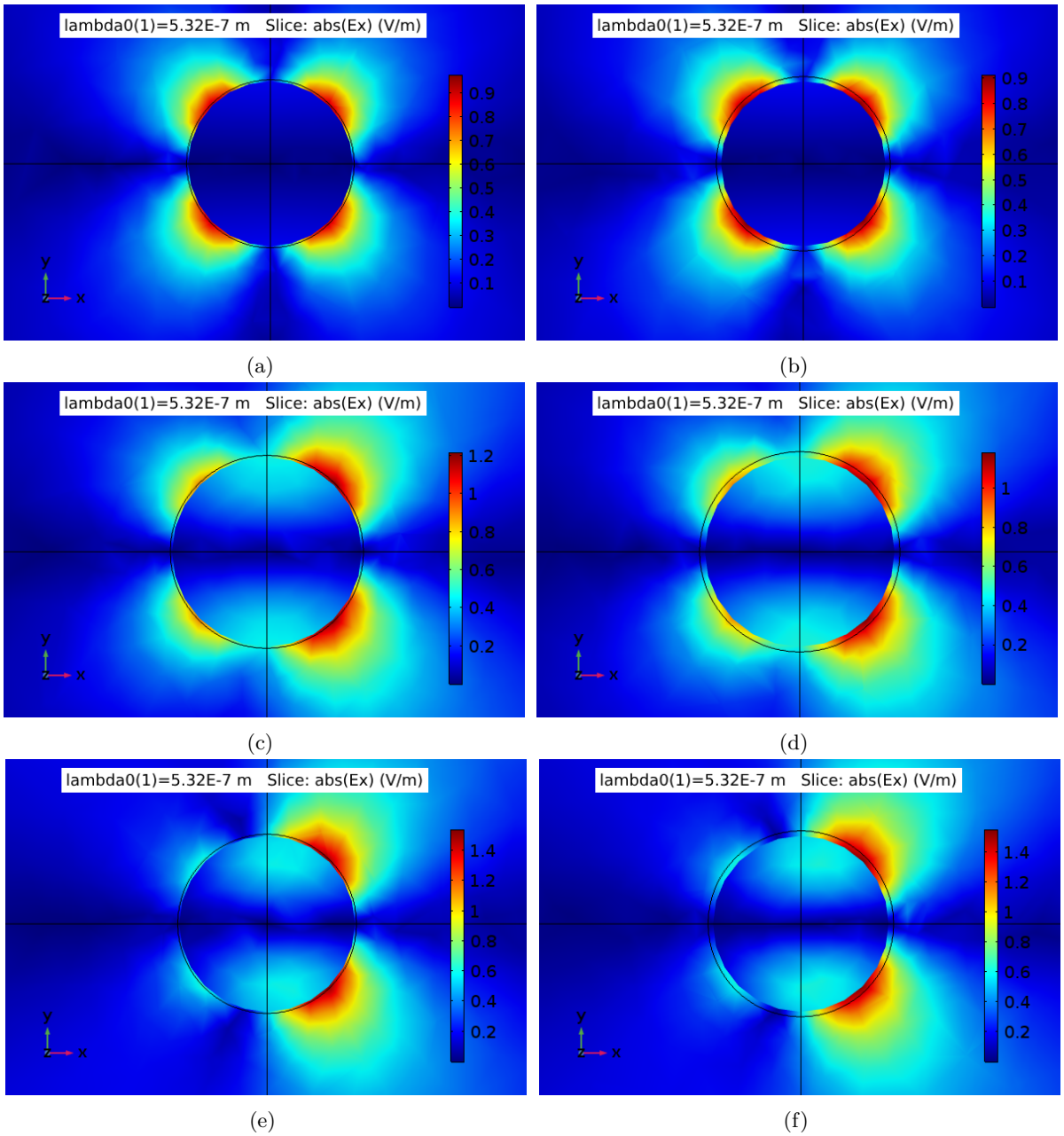

Figure 3.3: Color plot of the E_x field of (a, c, e) a 1 µm long nanowire and (b, d, f) a 3 µm long nanowire with a diameter of (a, b) 40, (b, c) 80 and (e, f) 100 nm. The values of E_x are represented by the color in all figures.

3.2 Scattering cross section per unit length

The scattering cross section per unit length was obtained for nanowires with different diameter and length (see fig. 3.4 and 3.5) using the DDA method (ch.2).

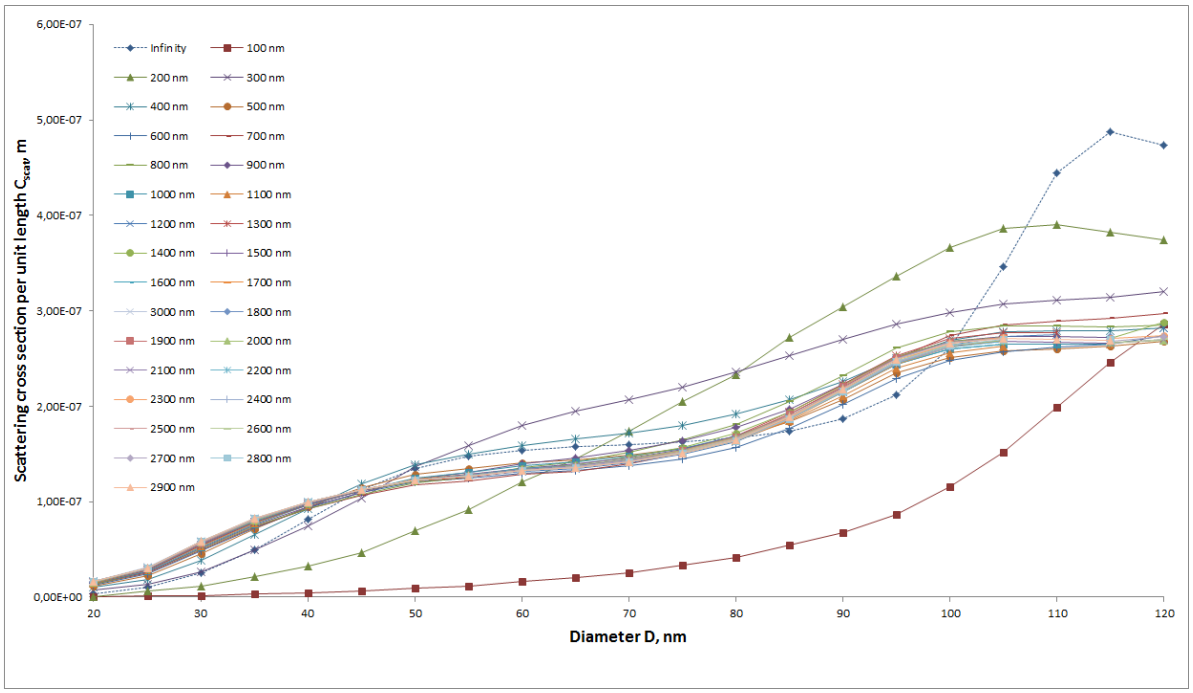

Figure 3.4: The cross section per unit length C_{scat}, calculated with DDScat vs. the diameter D for wavelength $\lambda = 532\,\text{nm}$ and different lengths L.

From fig.3.4, it can be deduced that the scattering cross section per unit length of the infinitely long nanowires does not correspond to the one of any finitely long nanowire in the range of the simulations. However, the scattering cross section per unit length can be approximated to constant for nanowires with length of 500 nm or more. If the scattering cross section per unit length is approximated to the one of a 2 µm long nanowire, the difference between the simulated cross section per unit length and the cross section per unit length for 2 µm long nanowire is at most 10% of the cross section per unit length for 2 µm long nanowire for 500 nm or longer nanowires.

Fig.3.5 shows that the scattering cross section per unit length at 2 µm is sufficient approximation for nanowires with length of at least 500 nm if their diameter is 35 nm or more.

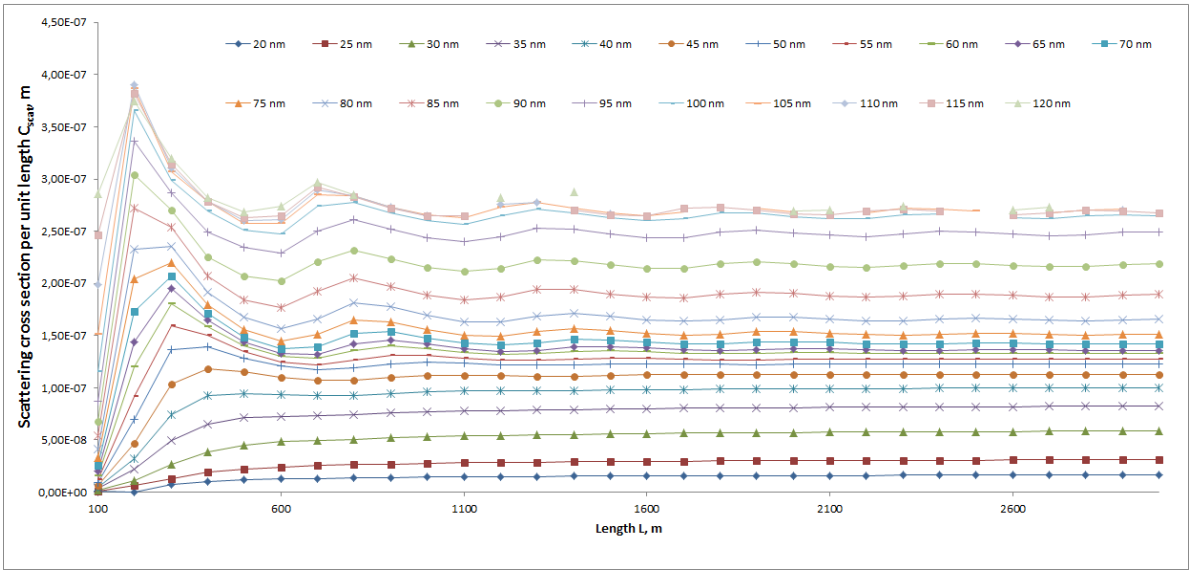

Figure 3.5: The cross section per unit length C_{scat} vs. the length L for $\lambda = 532\,\text{nm}$ and different diameters D.

3.3 Nanowire spectra

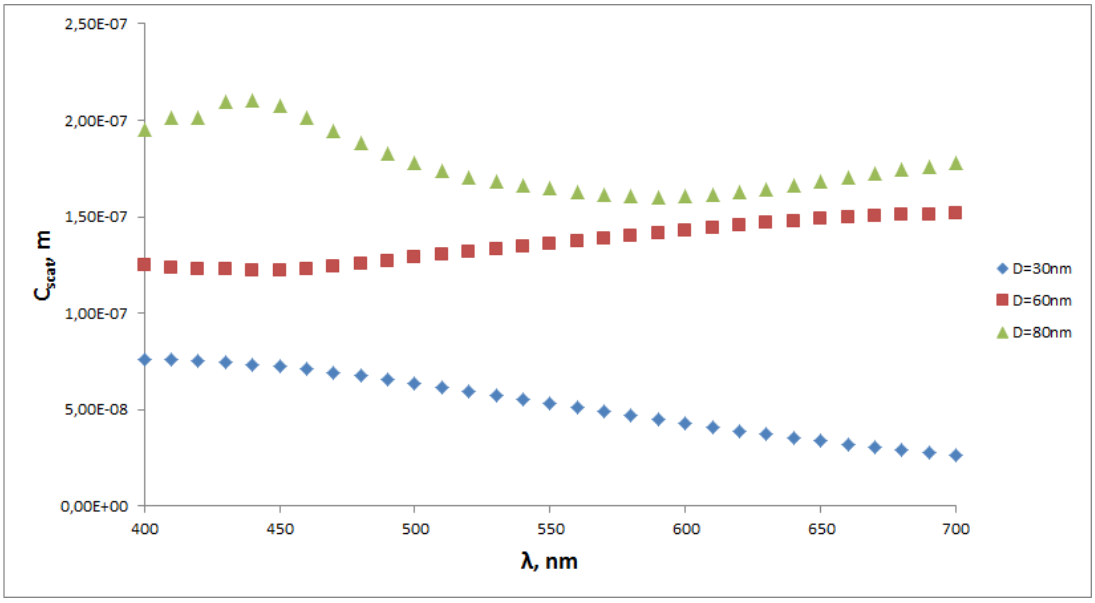

Figure 3.6: The spectra (cross section per unit length C_{scat} vs. wavelength of the incoming light λ) of 2 µm long nanowires with diameter of 30, 60 and 80 nm and refractive index $n = 4.1 + 0.32i$, simulated with DDScat.

The distribution of cross sections per unit length of nanowires with different radii and a refractive index $n = 4.1 + 0.32i$ (see table 3.1) were simulated with DDScat (see fig.3.6). They behave differently so no overall trend was observed; therefore, there was no opportunity for any simplification, since the diameter seems to be affecting the relationship between the wavelength and the cross section.

Chapter 4

Discussion and conclusion

The initial assumption of the thesis was that the scattering cross section per unit length of a nanowire with a certain diameter would converge to the scattering cross section per unit length of an infinitely long nanowire with the same diameter. That was not in complete agreement with the simulations. The cross section per unit length seemed to converge and be approximately constant for nanowires with length between 1 and 3 µm and with diameter bigger than 35 nm. However, it does not converge to the value for an infinitely long nanowire but to a value close to it. A possible reason is that the infinitely long nanowire model completely neglects the absorption, which is present in finitely long nanowires and seem to be consistent for all lengths tested. Moreover, the fluctuations observed in fig.3.5 are most likely due to Fabry-Perot resonances - the light scattered along the wire gets reflected at the ends, thus, resulting in interference, which alters the scattering cross section per unit length.

However, approximating the scattering cross section per unit length to the simulated one for a nanowire with the corresponding diameter and a length of 2 µm, gives relative error less than 10%. Moreover, the near-field patterns of finitely long nanowires with the same diameter and different length match much better than a finitely long and an infinitely long nanowire. This leads to the conclusion that for nanowires with length between 1 and 3 µm, length would not change the scattering cross section per unit length sufficiently, so that reduces the simulation parameters by one.

The spectra of a few nanowires with different diameter were obtained but there was no overall trend that could lead to possible simplification. The plot looked qualitatively like the spectrum on fig.1.2 but a quantitative description would require more research. For example, a different angle of incidence might result in weaker of stronger Fabry-Perot resonances and a different wavelength of the incident light will result in different refractive index, thus, different scattering and absorption cross sections.

Bibliography

[1] R.S. Wagner and W.C. Ellis. Vapor-liquid-solid mechanism of single crystal growth. *Applied Physics Letters*, 4(5):89–90, 1964.

[2] Continuous gas-phase synthesis of nanowires with tunable properties. *Nature*, (7427):90, 2012.

[3] InP nanowire array solar cells achieving 13.8% efficiency by exceeding the ray optics limit. *Science*, (6123):1057, 2013.

[4] Yang Chen, Mats-Erik Pistol, and Nicklas Anttu. Design for strong absorption in a nanowire array tandem solar cell. *SCIENTIFIC REPORTS*, 6, n.d.

[5] Y. (1) Chen, M.-E. (1) Pistol, N. (1) Anttu, O. (2) Höhn, and N. (2) Tucher. Optical analysis of a III-V-nanowire-array-on-Si dual junction solar cell. *Optics Express*, 25(16):A665–A679, 2017.

[6] L. Samuelson. Nanowire LEDs and solar cells. Lund University, Nanometer Structure Consortium, Lund, Sweden, 5193, 2014.

[7] Mohammad Karimi, Magnus Heurlin, Steven Limpert, Vishal Jain, Xulu Zeng, Irene Geijselaers, Ali Nowzari, Ying Fu, Lars Samuelson, Heiner Linke, Magnus T. Borgstrom, and Hakan Pettersson. Intersubband quantum disc-in-nanowire photodetectors with normal-incidence response in the long-wavelength infrared. *NANO LETTERS*, 18(1):365 – 372, n.d.

[8] Increased absorption in InAsSb nanowire clusters through coupled optical modes. *Applied Physics Letters III-V Nanowire Array Solar Cells: Optical and Electrical Modelling*, (8), 2017.

[9] Eleni Gompou. Optical imaging and spectroscopy of airborne nanowires. http://lup.lub.lu.se/student-papers/record/8906421, 2017. Student Paper.

[10] Gustav Mie. Beiträge zur optik trüber medien, speziell kolloidaler metallösungen. *Annalen der Physik*, 330(3):377–445.

[11] Donald R. Huffman Craig F. Bohren. *Absorption and scattering of light by small particles.* John Wiley & Sons Incorporated, New York, 1983.

[12] Milton Kerker. *The Scattering of Light and Other Electromagnetic Radiation*, volume 16. Academic Press, New York, 1969.

[13] Mats G. Larson and Fredrik Bengzon. *The finite element method : theory, implementation, and applications.* Texts in Computational Science and Engineering: 10. Heidelberg : Springer, cop. 2013, 2013.